Study of a_0 mesons in the reaction $pp \to d\,a_0^+ \to d\,K^+\overline{K}^0$ at ANKE

L. A. Kondratyuk, V. P. Tchernyshev
Institute of Theoretical and Experimental Physics,
117259 Moscow, Russia

Ye. S. Golubeva
Institute of Nuclear Research,
117312 Moscow, Russia

M. Büscher, O. W. B. Schult, H. Seyfarth, K. Sistemich
Institut für Kernphysik, Forschungszentrum Jülich,
D-52425 Jülich, Germany

H. Müller
Institut für Kern- und Hadronenphysik, Forschungszentrum Rossendorf
D-01314 Dresden, Germany

A. Kacharava
Laboratory of Nuclear Problems, Joint Institute of Nuclear Research
141980 Dubna, Russia

and the ANKE collaboration

Spokesman: V. P. Tchernyshev (`chernyshov@vitep3.itep.ru`)
Local contact: M. Büscher (`m.buescher@kfa-juelich.de`)

March 10, 1997

Abstract

We propose to measure the cross section of the reaction $pp \to d\,a_0^+ \to d\,K^+\overline{K}^0$ and the mass spectra of the $K^+\overline{K}^0$ system at energies $T_p = 2.52 \ldots 2.60$ GeV at COSY using the ANKE spectrometer and a frozen-pellet target. Within approx. one week of beam time we intend to collect a few thousand events of a_0^+ decays into $K^+\overline{K}^0$ at different energies between 2.52 and 2.60 GeV. The results will help to clarify whether the a_0^+ is a real resonance or a $K^+\overline{K}^0$ threshold cusp.

Contents

1 Introduction and physics motivation **3**

2 Model calculations **3**

3 Experimental program **7**

4 Experimental set-up **9**
- 4.1 Description of the apparatus 9
- 4.2 The ITEP frozen-pellet target 9
- 4.3 Angular and momentum acceptance 11
- 4.4 Counting rates 11
- 4.5 Missing mass resolution 14
- 4.6 Background 14

5 Requested time for measurements **16**

1 Introduction and physics motivation

The scalar meson sector plays a very important role in the physics of hadrons. Nevertheless, the structure of the lightest scalar mesons $a_0(980)$ and $f_0(980)$ is not completely understood yet (see e.g. [1, 2, 3, 4, 5] and references therein). They can be either $q\overline{q}$ or $qq\overline{qq}$ states, molecules or even vacuum scalars which are eye-witnesses of confinement [2]. Moreover, there is a strong mixing between the uncharged $a_0(980)$ and the $f_0(980)$ due to coupling to $K\overline{K}$ intermediate states [6]. Therefore, it is important to study the charged components of $a_0(980)$ which are not mixed with the $f_0(980)$ and preserve their original quark content. Until now the charged components of $a_0(980)$ were studied mainly in the $\eta\pi^+$ or $\eta\pi^-$ channels [7]. At the same time, data on the $K\overline{K}$ channel of a_0 decay are rather scarce. For example, the data from only one experiment [8], where decay of the $a_0(980)$ into $K\overline{K}$ was seen in $p\overline{p}$ annihilations through the $f_1(1285)$ resonance, are used for analysis by the Particle Data Group [7]. The resolution of the $K\overline{K}$ invariant mass in this experiment was 20 MeV. Such a poor resolution is not sufficient to solve the question whether the $a_0(980)$ is a real resonance or a cusp effect close to threshold [4].

Therefore, it is important to measure the $K\overline{K}$ decay channel of $a_0^+(980)$ or $a_0^-(980)$ with better resolution. Such conditions can be realized at COSY. We propose to study the $a_0^+(980)$ in the reaction

$$pp \to d\, a_0^+ \to d\, K^+ \overline{K}^0 \tag{1}$$

at ANKE. The measurement of the invariant mass of the $K\overline{K}$ system at different energies above the $K\overline{K}$ threshold will help to clarify whether the $a_0(980)$ is a real resonance or a $K\overline{K}$ threshold cusp or a $K\overline{K}$ molecule.

The study of the reaction (1) at COSY has the following advantages:

- the final $K\overline{K}$ system is produced in a pure isospin state $I = 1$. This prevents its mixing with the f_0 meson, which happens in neutral $K\overline{K}$ modes,
- the deuteron in the final state is preferable as compared with the unbound pn system due to a larger detection efficiency,
- because the maximal energy at COSY is only slightly above the threshold of $K\overline{K}$ production the cross section of reaction (1) is essentially larger than the cross section of the reaction with pn in the final state, which is suppressed much stronger by phase space.

2 Model calculations

In order to estimate the cross section of the reaction $pp \to d\, a_0^+ \to d\, K^+\overline{K}^0$ we use the guark-gluon string model (QGSM) which is a microscopic model for Regge phenomenology [9].

In [9, 10] QSGM was succesfully applied to the descripion of the reactions $pp \to d\,\pi^+$ and $\overline{p}d \to p\,\pi^-$. In this model the amplitudes of the reaction $pp \to d\,\pi^+$ and the line-reversed reaction $\overline{p}d \to p\,\pi^-$ can be described in first approximation by the contribution of the three valence-quark exchange in the t-channel (see Fig. 1) and are equal. This equality is a consequence of the line-reverse invariance, which is valid in QGSM. Therefore, by fitting the parameters of the model to the reaction $pp \to d\,\pi^+$ (see Fig. 2a) we can predict the cross section of the reaction $\overline{p}d \to p\,\pi^-$ (see Fig. 2b) and vice versa. Comparing Fig. 2a and b we see that the line-reverse invariance works rather well in this case.

Here we apply this method for a prediction of the cross section for the reaction $pp \to da_0^+$. We have to fix only one parameter: the ratio of the amplitudes $pp \to da_0^+$ and $pp \to d\pi^+$. Assuming the validity of the line-reverse invariance we can express this ratio through the ratio

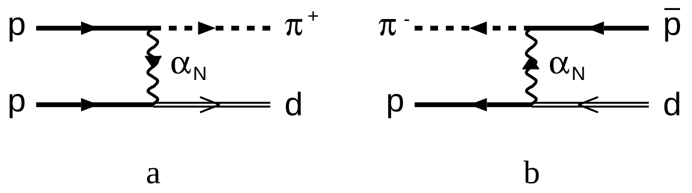

Figure 1: Exchange of a neutron-like Reggeon (three valence quarks udd) in the direct pp $\rightarrow$ d π^+ **a** and line-reversed $\overline{\mathrm{p}}$d $\rightarrow$ p π^- **b** reactions

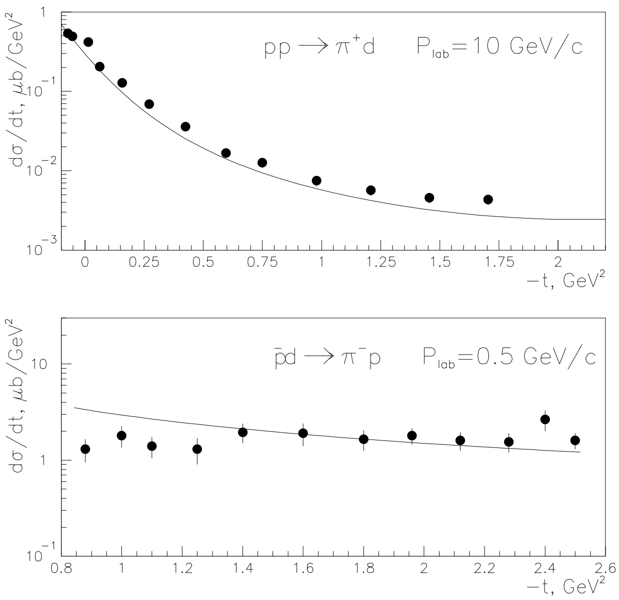

Figure 2: Differential cross sections of the reactions pp $\rightarrow$ d π^+ **a** and $\overline{\mathrm{p}}$d $\rightarrow$ p π^- **b**. The solid curves are calculated within the QGSM

of the amplitudes $\overline{\rm p}{\rm d} \to {\rm pa}_0^-$ and $\overline{\rm p}{\rm d} \to {\rm p}\pi^-$. The latter can be found using the calculations of the branching ratios for the Pontecorvo reaction $\overline{\rm p}{\rm d} \to {\rm pa}_0^-$, performed by Bussa et al. [11]. In Table 1 we show that the predictions of the branching ratios for different Pontecorvo reactions $\overline{\rm p}{\rm d} \to {\rm NM}$ within the framework of the relativistic two step model developed in [12] agree very well with the available experimental data of the Crystal Barrel and OBELIX collaborations [13, 14]. The calculated branching ratio of the reaction $\overline{\rm p}{\rm d} \to {\rm pa}_0^-$ presented in Table 1 is in agreement with preliminary data from OBELIX [15] which show comparable yields for ${\rm a}_0^0{\rm n}$ and $\phi{\rm n}$ production in $\overline{\rm p}{\rm d}$ annihilation at rest into ${\rm K}^+{\rm K}^-{\rm n}$.

Table 1: Branching ratios for different reactions $\overline{\rm p}{\rm d} \to {\rm NM}$ found in [11] in comparison with the experimental data of the Crystal Barrel and OBELIX collaborations [13, 14]

$\overline{\rm p}{\rm d} \to {\rm MN}$	Exp. BR in 10^{-6}	Theor. BR in 10^{-6}
$\pi^-{\rm p}$	12.9 ± 0.8	12.9 ± 0.7
$\eta{\rm n}$	3.19 ± 0.48	6.22 ± 0.6
$\eta'{\rm n}$	8.2 ± 3.4	5.95 ± 0.75
$\rho^-{\rm p}$	29.0 ± 7.0	31.1 ± 3.4
$\omega{\rm n}$	22.8 ± 4.1	17.0 ± 0.3
$\phi{\rm n}$	2.7 ± 0.5	1.7 ± 0.3
${\rm a}_0^-{\rm p}$	?	$6\ldots12$

In Fig.3 we present the cross sections of the reactions ${\rm pn} \to {\rm d}\phi$ and ${\rm pp} \to {\rm da}_0^+$ calculated within this approach. We used branching ratios ${\rm BR}(\overline{\rm p}{\rm d} \to {\rm N}\phi) = 2 \cdot 10^{-6}$ and ${\rm BR}(\overline{\rm p}{\rm d} \to {\rm pa}_0^-) = (9 \pm 3) \cdot 10^{-6}$. The cross section of the reaction ${\rm pn} \to {\rm da}_0^0$ is expressed through the cross section of reaction (1) using isotopic invariance. If there is strong mixing of ${\rm a}_0$ and ${\rm f}_0$ ([6]) then the isotopic invariance will be violated in this case. From Fig.3 it can be seen that at the maximum energy for COSY $T_{\rm p} = 2.60$ GeV ($p_{\rm p} \approx 3.4$ GeV/c) the cross section of reaction (1) is about (0.33 ± 0.11) μb. This value is in agreement with the cross section found within the framework of the Rossendorf-Collision Model [16, 17] which predicts $\sigma({\rm p}(2.6~{\rm GeV}){\rm p} \to {\rm da}_0^+) \approx 0.3$ μb.

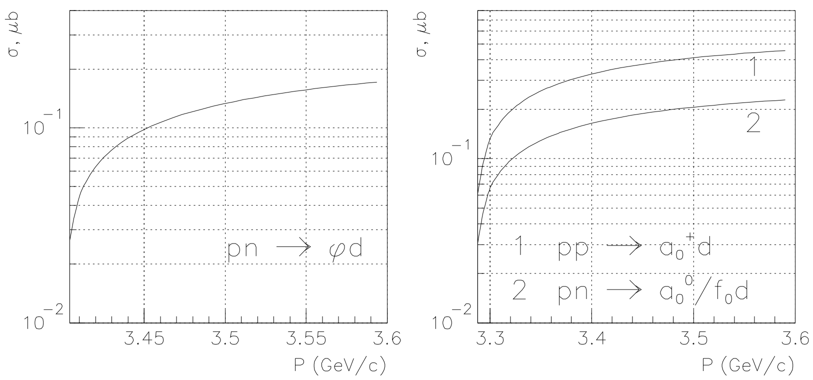

Figure 3: Total cross sections of the reactions ${\rm pn} \to {\rm d}\phi$, ${\rm pp} \to {\rm da}_0^+$ and ${\rm pn} \to {\rm da}_0^0$ calculated within the QGSM

In Fig.4 we present the missing-mass spectrum of a_0^+ mesons $M(a_0^+) = MM(\mathrm{pp}, \mathrm{d})$ at $T_\mathrm{p} = 2.52$ GeV and $T_\mathrm{p} = 2.60$ GeV. We compare two different approaches for the description of the a_0 peak, seen by the Crystal Barrel collaboration [18] in $\eta\pi^0$ invariant mass from $\overline{\mathrm{p}}\mathrm{p}$ annihilation at rest: i) Breit-Wigner distribution with $M_\mathrm{R} = 982$ MeV and $\Gamma_\mathrm{R} = 54$ MeV [18]; ii) Flatte distribution [5]. Both approaches give an equally good description of the Crystal Barrel data on $M(\eta\pi^0)$, because the sharp peak in the Flatte distribution is smoothed by the experimental mass resolution. In our case the shapes of the mass distributions are essentially different for cases i) and ii) at $T_\mathrm{p} \leq 2.60 GeV$ because of the strong influence of the threshold cut at higher masses, compare Fig. 4a and b.

The $\mathrm{K}^+\overline{\mathrm{K}}^0$ invariant mass distributions for case i) are shown in Fig.5 a at different T_p. They are cut by the threshold effect at higher masses and by the $\mathrm{K}\overline{\mathrm{K}}$ phase space at lower masses. Those cuts cause a rather strong energy dependence of the cross section of reaction (1) which is equal to $8.35 \cdot 10^{-4}$, $7 \cdot 10^{-3}$ and $1.7 \cdot 10^{-2}$ μb at 2.52, 2.56 and 2.60 GeV, respectively.

The shape of the $\mathrm{K}^+\overline{\mathrm{K}}^0$ mass distribution is model dependent. In Fig.5 b we present $\mathrm{d}\sigma/\mathrm{d}M$ for case i) at two different values of $\Gamma_\mathrm{R} = 54$ and 100 MeV and for the Flatte distribution (case ii)) normalised to the BW case with $\Gamma_\mathrm{R} = 54$ MeV. The positions of the maxima of the solid and dotted curves are shifted by 15 MeV. The dashed curve is rather smooth. As the mass resolution in our case is expected to be about 7 MeV (see chapter 4.5), all three presented shapes of $\mathrm{d}\sigma/\mathrm{d}M$ can be distinguished.

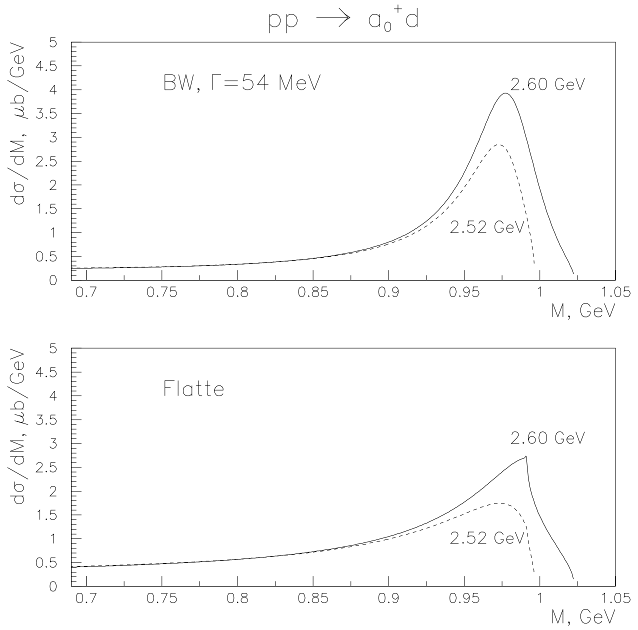

Figure 4: Missing-mass spectrum $MM(\mathrm{pp}, \mathrm{d})$ for the reaction $\mathrm{pp} \to \mathrm{d}a_0^+$ at different beam energies for the Breit-Wigner approach **a** and a Flatte distribution **b**

Reaction (1) can be identified detecting the deuteron and the K^+ meson. The main goal will be to measure the cross section of reaction (1) and the mass spectra of the $\mathrm{K}^+\overline{\mathrm{K}}^0$ system at different energies. If the a_0 is a molecule or a threshold cusp some narrow structure in $\mathrm{d}\sigma/\mathrm{d}M$ should appear at small masses and it will not change much with increasing beam energy from 2.52 to 2.60 GeV. However, if it is a genuine resonance the shape of the peak

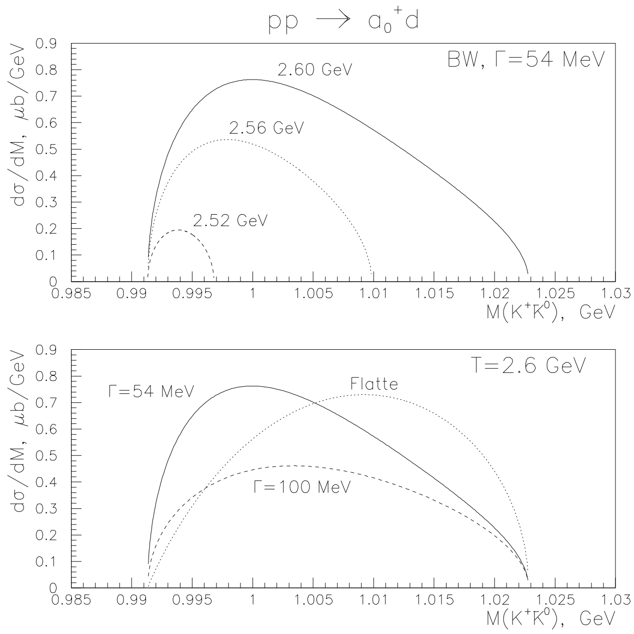

Figure 5: Invariant mass spectrum $M(\mathrm{K}^+\overline{\mathrm{K}}^0)$ for the reaction pp $\rightarrow$ da_0^+ at different energies for the Breit-Wigner approach **a** and for various shapes of the a_0 peak at T_p = 2.6 GeV **b**

will change as it is shown in Fig.5 **b** for the BW case or Flatte distribution.

In Fig.6 we present the momentum and angular distributions of deuterons and kaons at T_p = 2.52 and 2.60 GeV. The maximum of the momentum distribution is near 2.2 GeV/c for deuterons and near 0.6 GeV/c for kaons. The angular distribution for deuterons and kaons (only for T_p = 2.52 GeV) is forward peaked at $\vartheta \leq 8°$. At T_p = 2.6 GeV the kaons have a broader angular distribution with a maximum at $\vartheta = 6 \ldots 10°$.

3 Experimental program

We intend to study the a_0^+ production in the reaction pp $\rightarrow$ d a_0^+ $\rightarrow$ d $\mathrm{K}^+\overline{\mathrm{K}}^0$ at different beam energies between T_p = 2.52 and 2.60 GeV. We propose to start with the measurement of the cross section of reaction (1) and the shape of the $\mathrm{K}^+\overline{\mathrm{K}}^0$-mass distribution. This is possible by simultaneously measuring the deuteron and K^+ momenta and angles. The 4-momenta of the $\overline{\mathrm{K}}^0$ mesons can be reconstructed by a missing mass analysis. The structure of the a_0^+ meson can then be investigated by analyzing the invariant mass of the $\mathrm{K}^+\overline{\mathrm{K}}^0$ system. In principle, the inclusive measurement of deuterons would also allow the reconstruction of the a_0^+ mass. However, according to our estimates in the inclusive case the background of deuterons from channels not related to a_0^+ production is more than two orders of magnitude stronger and makes such an inclusive study impossible.

As the first measurement it seems useful to measure inclusive deuteron spectra from the reaction pp $\rightarrow$ dX since here the counting rates are larger and valuable information about the background conditions can be obtained in relatively short beam times. These kind of measurements have already been described in [19] and will be a part of the commissioning of the detection systems at ANKE.

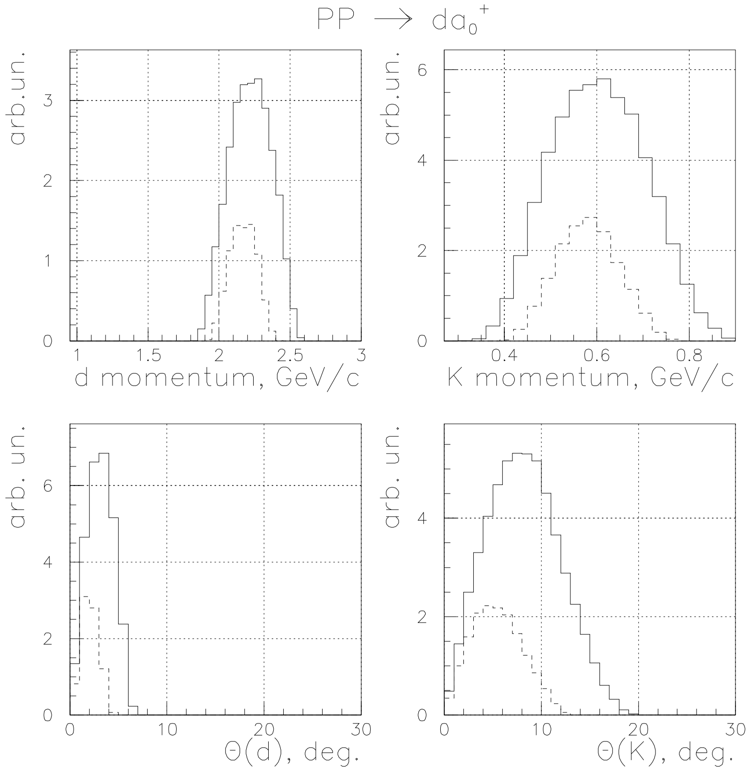

Figure 6: Mometum and angular distributions of deuterons and kaons from the reaction $pp \to da_0^+ \to dK^+\overline{K}^0$ at $T_p = 2.52$ GeV (dashed line) and $T_p = 2.60$ GeV (solid line)

After the study of the a_0^+ meson described here it is also foreseen to measure the production of the neutral mesons f_0 and a_0^0 in proton-neutron reactions ($pn \to da_0/f_0$) using deuterons as target material.

4 Experimental set-up

4.1 Description of the apparatus

The ANKE spectrometer [20] (see Fig.7) will allow to measure simutaneously positively and negatively charged particles emitted under forward angles $\leq 10°$. For the detection of K^+ mesons and deuterons and for the reduction of the background the following concept is suggested.

The K^+ mesons will be detected in the side detection system [21, 22] which will offer a K^+-detection efficiency of $\sim 10\%$ (including decay-in-flight between detectors and target) and a background supression (pions, protons and ejectiles scattered at the magnet iron) of more than 5 orders of magnitude [22, 23, 24, 25, 26] in the momentum range between 150 and 600 MeV/c. It allows to select events where a K^+ meson is produced with almost no background from other reaction channels. Kaons from a_0^+ decay have momenta in the range 400...800 MeV/c (Fig.6). Thus, the momentum acceptance of ANKE is about 50%. The angular distributions of kaons are also shown in Fig.6. If the primary proton-beam energy will be about 2.52 GeV practically all K^+ mesons are emitted into the forward angle cone $\vartheta \leq 10°$ and can be detected at ANKE.

The forward detector which is located between D2 and D3 will detect positively charged particles with momenta between 1.0 and 3.2 GeV/c [27]. At beam energies below 2.6 GeV deuterons from reaction (1) are emitted into a narrow forward cone with typical momenta around 2.2 GeV/c (Fig.6). Thus, they can be detected in the ANKE forward detector. According to simulation calculations the deuteron detection efficiency is $\sim 40\%$ and the background (mainly fast protons) suppression is about three orders of magnitude.

We conclude that the kinematical features of the process to be studied match the abilities of the ANKE set-up and that the detection systems will allow to identify reaction (1) with only very little background from other reaction channels by measuring K^+ mesons and deuterons.

4.2 The ITEP frozen-pellet target

Since we should be able to measure rather small cross sections $\sigma \approx 0.01\ldots0.1\mu b$ it is necessary to work at maximum luminosity. According to the time resolution of the ANKE detectors luminosities up to $L_{\max} \approx 10^{33}\ \mathrm{sec}^{-1}\,\mathrm{cm}^{-2}$ can be used.

In order to achieve such high luminosities an effective target thickness of $d \approx 10^{16}$ atoms cm^{-2} at a proton beam intensity $n \approx 10^{11}$ is desirable. Since we plan to study meson production in pp and pn collisions, the target material should be hydrogen or deuterium. The only device which fulfills these requirements is a frozen-pellet target. Such a target is currently being built at ITEP and could be ready for operation at ANKE in 1999; its properties are listed in Table 2.

The pellet-target systems in ITEP were developed during 1992–1993. Since 1994 part of the equipment has been fabricated and an infrastructure for target tests has been prepared. A scheme of the target is shown in Fig.8. There are the following operational conditions for the pellet target developed at ITEP.

- The target can make available different kinds of target nuclei. For the measurements proposed here H_2 and D_2 will be used.
- The diameter of the spherical pellets can be varied between 20 and 100 μm.

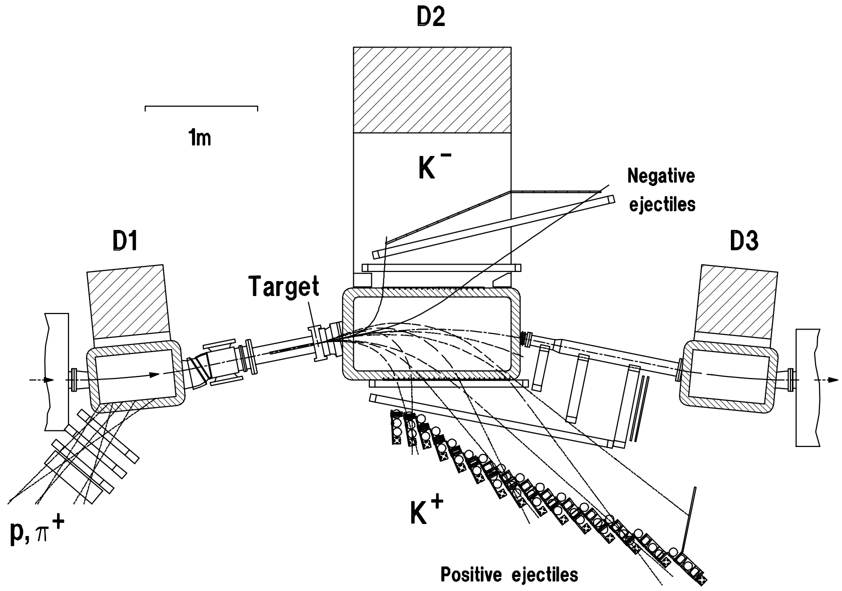

Figure 7: Layout of the setup at the ANKE spectrometer

Table 2: Densities of the ITEP frozen-pellet target with hydrogen as target material, a COSY-beam diameter of 2 mm, a beam intensity of $n = 3 \cdot 10^{10}$ and under the assumption that one pellet is in the beam

Diameter of pellet (μm)	Mass (g)	Total number of atoms per pellet	Luminosity (cm^{-2}s^{-1})
20	$3 \cdot 10^{-10}$	$1.8 \cdot 10^{14}$	$2.8 \cdot 10^{32}$
40	$2.3 \cdot 10^{-9}$	$1.4 \cdot 10^{15}$	$2.2 \cdot 10^{33}$
60	$8 \cdot 10^{-9}$	$4.8 \cdot 10^{15}$	$7.4 \cdot 10^{33}$

- The deviations of the pellet sizes is expected to be not more than 10%.
- The deviation of the pellet tracks in the horizontal plane is smaller than 100 μm.
- The flow rate of liquid Helium during the measurements is not higher than 1.5 liters per hour. The flow rate of liquid Nitrogen does not exceed two liters per hour.

It is foreseen to build the target such that as much existing equipment as possible (e.g. pumps and vacuum chambers of the Münster cluster-jet target for ANKE) can be used. A close collaboration with the target group from the University of Münster has been agreed upon.

4.3 Angular and momentum acceptance

With the ANKE detection systems positively charged particles in the momentum range $p_+ = 150\ldots 3200$ MeV/c can be measured. Ejectiles with vertical emission angles between $\pm 8^\circ$ ($p \approx 150$ MeV/c) and $\pm 3.5^\circ$ ($p > 550$ MeV/c) can be detected. The K^+ mesons will be identified with the side-detector system which will offer a horizontal acceptance of $-10^\circ < \vartheta < 10^\circ$. Fast deuterons with momenta up to $p_{\max} \approx 3.2$ GeV/c will be detected in the forward detection system. Horizontal emission angles in the range $\vartheta \approx -1\ldots 10^\circ$ can be detected.

In Fig.9 the effect of the angular and momentum acceptance of ANKE on the measured K^+ and deuteron spectra is illustrated. In the lower part of the figure the calculated distributions are folded with the acceptance for the detection of K^+/d pairs in coincidence. From a comparison of the two momentum spectra in Fig.9 it can be concluded that the geometrical acceptance of ANKE for the detection of K^+/d pairs is $\epsilon \approx 9\%$. If one takes into account that $\sim 70\%$ of the kaons decay in flight between the target and the telescopes and that the detection efficiency in the detectors is $\sim 35\%$ for kaons and $\sim 90\%$ for deuterons, the total probability to detect a K^+/d pair is

$$\epsilon(\mathrm{K}^+, \mathrm{d}) \approx 0.8\% \ .$$

We also calculated the detection efficiency for the inclusive measurement of deuterons from the reaction $\mathrm{pp} \rightarrow \mathrm{da}_0^+$ at $T_\mathrm{p} = 2.60$ GeV. In this case we expect:

$$\epsilon(\mathrm{d}) \approx 40\% \ .$$

4.4 Counting rates

For a detailed study of particle spectra we plan to observe about 10^3 a_0^+ decays into $\mathrm{K}^+\overline{\mathrm{K}}^0$ according to reaction (1) at different beam energies between 2.52 and 2.60 GeV. The predicted total cross section for $\mathrm{K}^+\overline{\mathrm{K}}^0$ production via the a_0^+ meson is about $\sigma_{\mathrm{tot}} \approx 0.017$ μb at $T_\mathrm{p} = 2.60$ GeV (see Sect. 2). In order to minimize background we shall detect coincident deuterons and K^+ mesons from a_0^+ decay. Thus, for a luminosity of 10^{32} $\mathrm{cm}^{-2}\mathrm{s}^{-1}$ (pellet target) the expected rate to observe an a_0^+ meson via its decay into $\mathrm{K}^+\overline{\mathrm{K}}^0$ is about:

$$\dot{n}(\mathrm{K}^+, \mathrm{d}) = \sigma \cdot \epsilon(\mathrm{K}^+, \mathrm{d}) \cdot L \approx 0.017 \cdot 10^{-30} \cdot 0.8 \cdot 10^{-2} \cdot 10^{32} = 0.014\ \mathrm{s}^{-1}$$

or ~ 50 events per hour. Since about 10^3 a_0^+ shall be detected ~ 20 hours of production beam time will be needed at $T_\mathrm{p} = 2.60$ GeV. At lower energies longer beam times will be needed in order to collect sufficient statistics.

In order to confirm the counting rate extimates described in this chapter we have also performed detailed GEANT simulations (for illustration see also e.g. [16] and Fig. 10) including a realistic 3 dimensional description of the magnetic field in D2. Within statistical uncertainties the results agree with the estimates given above.

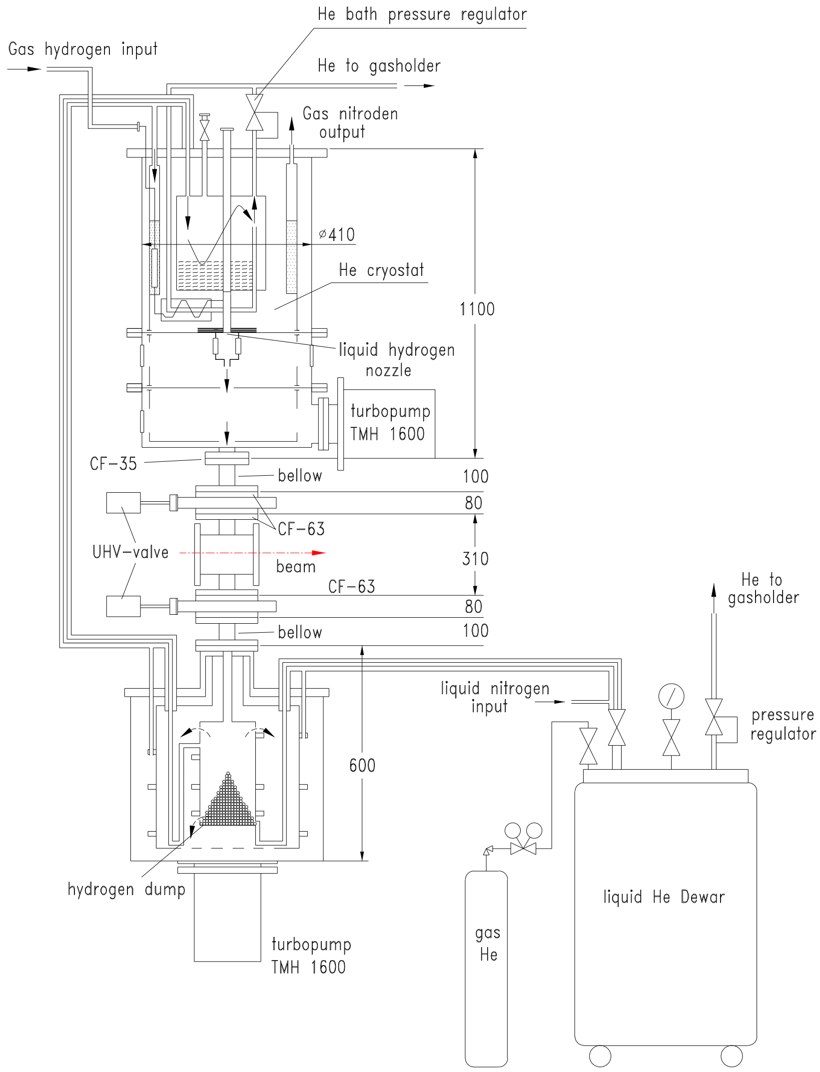

Figure 8: Layout of the ITEP frozen-pellet target

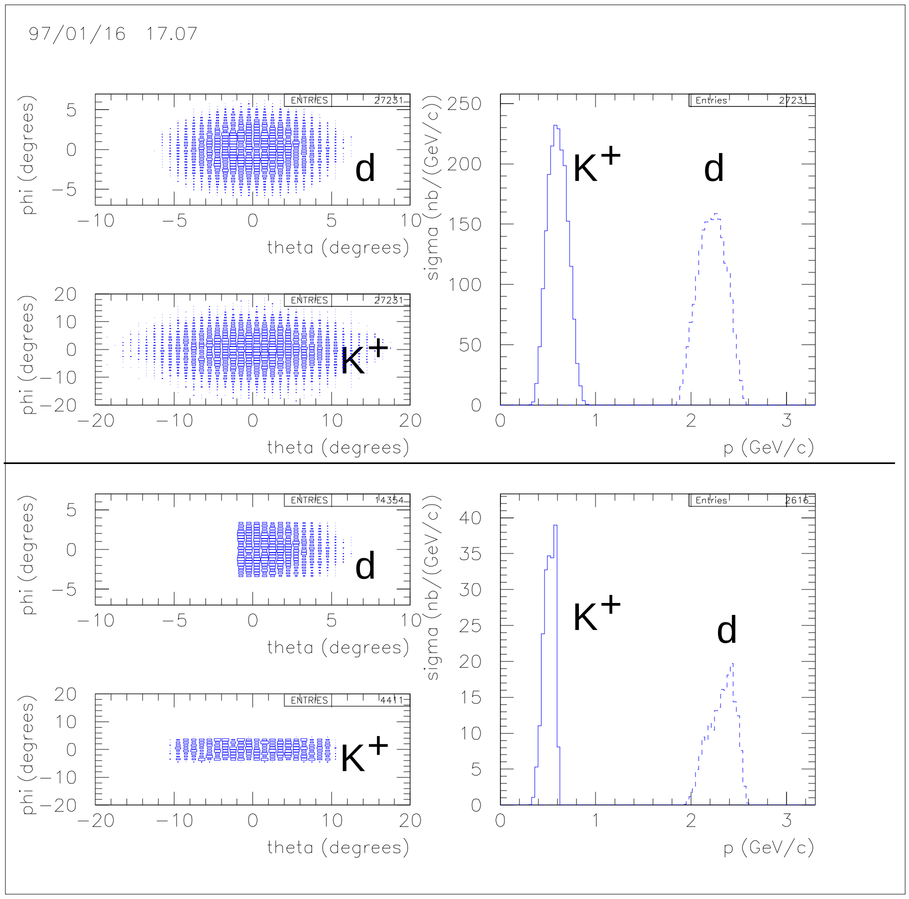

Figure 9: Angular (left) and momentum (right) distributions of K^+ mesons and deuterons from the reaction $pp \to da_0^+ \to dK^+\overline{K}^0$ at $T_p = 2.52$ GeV. The upper part of the figure shows the distributions calculated with the QGSM, in the lower part the angular and momentum acceptance of ANKE is taken into account

4.5 Missing mass resolution

The extraction of information on the structure of the a_0^+ meson requires a good resolution of the reconstructed a_0^+ mass. The accuracy should be in the range of a few MeV/c^2 (see also Fig. 5). We have performed GEANT simulations taking into account the particle propagation through D2, multiple scattering and energy losses in vacuum foils and detector components as well as the uncertainties of the track reconstruction procedure. Figure 10 shows the simulated tracks of K^+/d pairs which can be detected at ANKE. The simulation yields 'measured' track coordinates from the wire chamber information which allows to reconstruct the ejectile momenta at the target and, thus, the calculation of missing mass spectra.

Figure 11 shows the result of the calculations. The a_0^+ mass has been reconstructed from the measured tracks of the emitted deuterons according to the formula:

$$M(\mathrm{a}_0^+) = MM(\mathrm{pp,d}) = (\mathcal{P}_{\mathrm{P_P}} + \mathcal{P}_{\mathrm{P_T}} - \mathcal{P}_{\mathrm{d}})^2 \ ,$$

where $\mathcal{P}_{\mathrm{P_P}}$, $\mathcal{P}_{\mathrm{P_T}}$ are the known 4-momenta of the projectile and target protons and $\mathcal{P}_{\mathrm{d}}$ the measured 4-momentum of the deuteron. It is known from earlier simulations that the momentum resolution for the measurements of deuterons with the forward detector is $\Delta p/p \approx 1.5\%$ (FWHM).

From the right plot in Fig. 11 we conclude that the accuracy of the reconstructed a_0^+ mass ($\Delta m/m \approx 7$ MeV/c^2 (FWHM)) will be good enough to draw conclusions about the structure of this meson.

4.6 Background

For the study of reaction (1) the K^+ mesons will be detected in coincidence with deuterons and the a_0^+ will be reconstructed from the missing mass distribution MM(pp,d). We can expect the following background reactions during this experiment:

$$\mathrm{pp} \to \mathrm{d\,K^+\overline{K}^0}, \tag{2}$$

non-resonant production, and

$$\mathrm{pp} \to \mathrm{p\,K^+X} \ , \tag{3}$$

with misidentification of the proton as a deuteron.

Non-resonant $\mathbf{K^+\overline{K}^0}$ production: The non-resonant $K^+\overline{K}^0$ production is expected to be rather small. We estimate it as follows: First we take the parametrization of the cross section of the reaction

$$\mathrm{pp} \to \mathrm{pp\,K^+K^-} \tag{4}$$

from [28] $\sigma_{\mathrm{K^+K^-}} = A(1 - s_0/s)^3(s_0/s)^{0.8}$ where $\sqrt{s_0}$ is the threshold c.m. energy, $A = 0.8$ mb. This value of A can be found using the data $\sigma_{\mathrm{exp}} = (12\pm3)\ \mu$b at $p_{\mathrm{lab}} = 4.95$ GeV/c. At 6 MeV above threshold this model predicts $\sigma_{\mathrm{K^+K^-}} \approx 60$ pb which is in reasonable agreement with preliminary data from COSY 11 [29]. At 32 MeV above threshold ($T_{\mathrm{p}} \approx 2.6$ GeV) we have $\sigma \approx 10^{-3}\mu$b which is essentially lower than the cross section of reaction (1) at the same energy. The main reason is the very sharp threshold behaviour of $\sigma_{\mathrm{K^+K^-}} \propto A(1 - s_0/s)^3$. On the other hand the threshold behaviour of σ for the quasi two-body reaction (1) is $\sigma_{\mathrm{da_0^+}} \propto (1 - s_0/s)^{0.5}$.

We have assumed that the cross section of the reaction

$$\mathrm{pp} \to \mathrm{pn\,K^+\overline{K}^0} \tag{5}$$

is two times larger which is valid in the one-pion exchange model. Then we have calculated $d\sigma/dM$ in the OPE model for a relative energy of the pn pair of less than 5 MeV and found

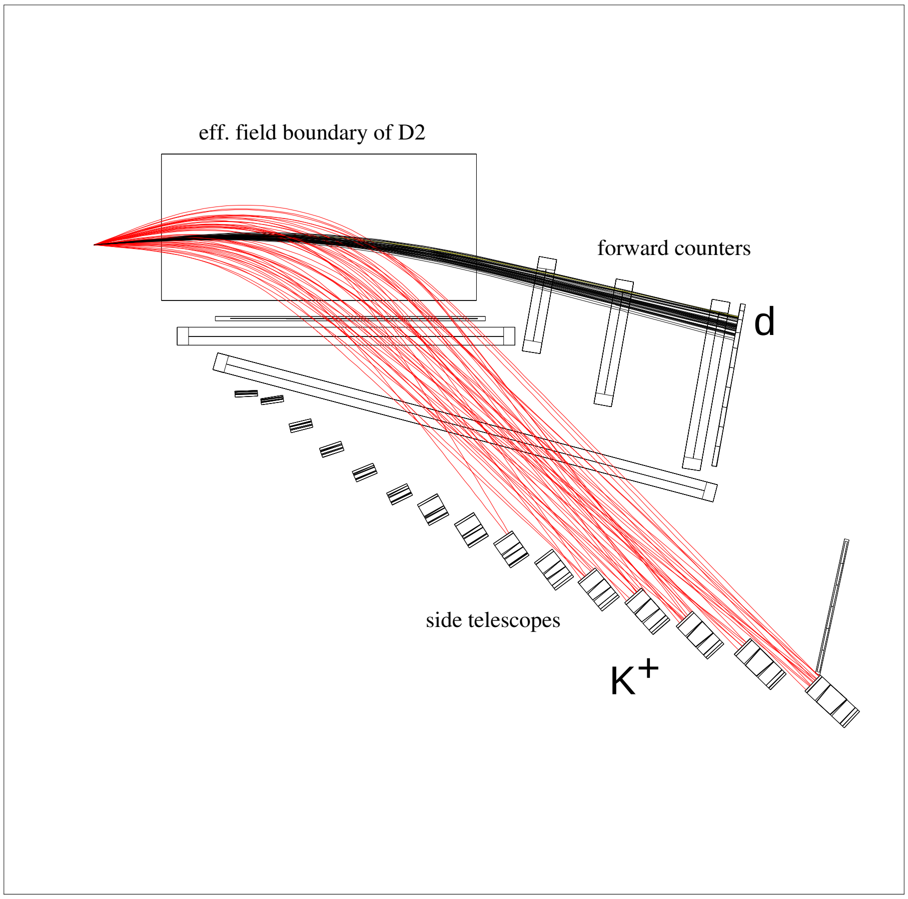

Figure 10: Tracks of 50 correlated K^+ mesons and deuterons from the reaction $pp \to da_0^+ \to dK^+\overline{K}^0$ at $T_p = 2.52$ GeV which are detected in the side and forward detectors

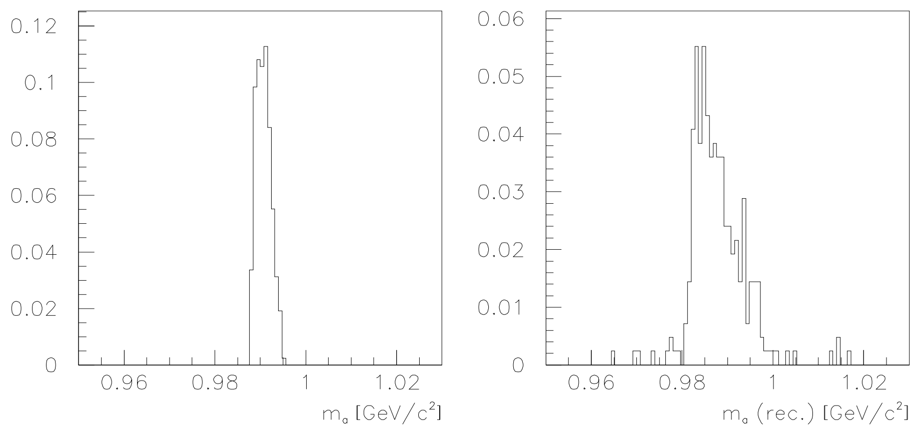

Figure 11: Missing mass $MM(\mathrm{pp,d})$ of deuterons from the reaction $\mathrm{pp} \to \mathrm{da}_0^+ \to \mathrm{dK}^+\overline{\mathrm{K}}^0$ at $T_\mathrm{p} = 2.52$ GeV. The left side of the figure shows the mass distribution from Fig. 5 folded with the acceptance of ANKE and measured with perfect resolution. In the right plot multiple scattering, energy losses and the uncertainties of the track reconstruction have been taken into account

$\mathrm{d}\sigma/\mathrm{d}M \leq 0.5 \cdot 10^{-3}$ μb/GeV at $M = 1$ GeV. This cross section is approximately three orders of magnitude smaller than for reaction (1), see Fig. 5. Therefore, the nonresonant background can be neglected.

Proton misidentification: The proton momentum spectrum for the reaction $\mathrm{pp} \to \mathrm{p}\Lambda\mathrm{K}^+$ and emission angles $\vartheta < 10°$ is rather flat for momenta 1.5 . . . 2.5 GeV/c, see Fig. 12. We obtained

$$\left(\frac{\mathrm{d}\sigma}{\mathrm{d}\Omega\mathrm{d}p}\right)_\mathrm{p} \approx 40\ \mu\mathrm{b/(sr\,GeV/c)}\ . \tag{6}$$

According to our calculations with the Rossendorf-Collision Model all other channels of K^+ production can increase the proton yield not more than by a factor of two.

From the deuteron momentum spectrum shown in Fig. 12 we found for deuterons with momenta 2.0 . . . 2.5 GeV/c:

$$\left(\frac{\mathrm{d}\sigma}{\mathrm{d}\Omega\mathrm{d}p}\right)_\mathrm{d} \approx 1\ \mu\mathrm{b/(sr\,GeV/c)}\ . \tag{7}$$

Therefore, the expected d/p ratio at $p \approx 2.2$ GeV/c is about $n(\mathrm{d})/n(\mathrm{p}) \approx 10^{-2}$.

According to our GEANT simulation calculations of the p/d discrimination in the forward detector, these counters will suppress protons by at least three orders of magnitude whereas the deuteron detection efficiency is higher than 80%. This high proton suppression can be achieved with tilted Čerenkov counters based on the principle of total internal reflection [30]. These counters offer an on-line proton suppression by more than two orders of magnitude. Additionally, in an off-line analysis of the TOF between the target and forward counter (start time at the target obtained from the reconstruction of the K^+ tracks) an additional suppression by more than one order of magnitude will be possible [22].

5 Requested time for measurements

We propose to start the study of the scalar mesons structure with the measurement of the background conditions. At the first stage of experiment we plan to measure the missing mass

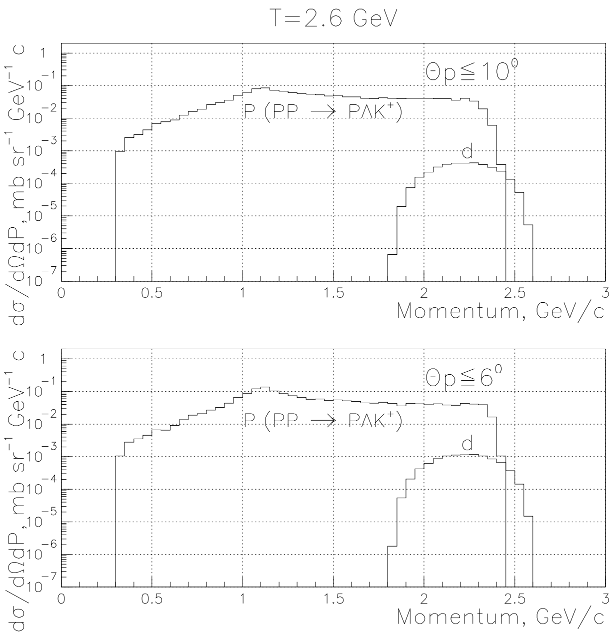

Figure 12: Calculated momentum spectrum of protons from the reaction p(2.6 GeV)p $\to$ pΛK$^+$ and deuterons from reaction (1) with emission angles $\vartheta < 10°$ **a** and $\vartheta < 6°$ **b**

distribution for the inclusive reaction pp $\to$ dX$^+$ at $T_{\rm p} \approx 2.6$ GeV. Then we want to measure deuterons and K$^+$ mesons from the reaction pp $\to$ d $a_0^+ \to$ d K$^+\overline{\rm K}^0$.

Summarizing, we apply for the following amount of beam time:

- One week for calibration measurements and background studies using a target with relatively low luminosity e.g. a cluster-jet target as soon as the detectors for K$^+$ mesons and fast deuterons are available at ANKE (Middle of 1998). These measurements will allow to calibrate the p/d suppression in the Čerenkov counters.
- One week for the invariant mass measurements when the frozen-pellet target will be ready (End of 1999).

In a later stage of the proposed studies it is also planned to apply for beam time to measure the reactions pn $\to$ dX using the frozen-pellet target.

Acknowledgements

We are very grateful to W. Cassing, C. Guaraldo, U. Mosel and J. Speth for useful discussions and to W. Oelert for providing us the cross section of the reaction pp $\to$ pp K$^+$K$^-$ near threshold.

References

[1] J. Weinstein, Proc. Int. Conf. on Particle Production near Threshold, Nashville, U.S.A., 1990, Particles and Fields Series 41, H. Nann and E. J. Stephenson, Edts., AIP, New York (1991) p.256.

[2] F.E.Close et al., Phys.Lett.**B 319** (1993) 291.

[3] M.Genovese et al., Nuovo Cim.**107A** (1994) 1249.

[4] G.Janssen, B.Pierce, K.Holinde and J.Speth, Phys.Rev.**D 52** (1995) 2690.

[5] V.V.Anisovich et al., Phys.Lett.**B 355** (1995) 363.

[6] J. Speth, *private communication.*

[7] R.M.Barnett et al. (Particle Data Group), Phys.Rev.**D 54** (1996) 1.

[8] L.de Billy et al., Nucl.Phys.**B 176** (1980) 1.

[9] A.B.Kaidalov, Sov.J.Nucl.Phys.**53** (1991) 872.

[10] C.Guaraldo, A.B.Kaidalov, L.A. Kondratyuk and Ye.S. Golubeva, Proc. of the 3rd Int. Conf. on Nucleon-Antinucleon Physics (NAN'95), Phys. of Atomic Nuclei **59** (1996) 1832.

[11] M.P.Bussa, Ye.S.Golubeva,C.Guaraldo,L.A.Kondratyuk and L.Valacca, *in preparation.*

[12] L.A.Kondratyuk and C.Guaraldo, Phys.Lett.**B 256** (1990).

[13] C.Amsler et al., Physics of Atomic Nuclei**59** (1996) 1473.

[14] V.G.Ableev et al., Nucl.Phys.**A 562** (1993) 617.

[15] M.Bussa and P.Cerello, *private communication.*

[16] H.Müller et al., COSY Proposal #21: Study of K^- production (1996).

[17] H.Müller, Z.Phys.**A 339** (1991) 409.

[18] C. Amsler et al., Phys.Lett.**B 291** (1992) 347.

[19] V.Koptev et al., COSY Proposal #38: NN Final-State Interactions in Single Pion Production (1996).

[20] O.W.B.Schult et al., IKP-KFA Annual Report 1992, p.11 (1993).

[21] A.Franzen, M.Büscher, IKP-KFA Annual Report 1994, p.57 (1995).

[22] M.Büscher et al., Communication of the JINR, Dubna 1996.

[23] M.Büscher et al., Z.Phys.**A 355** (1996) 93.

[24] M.Büscher and H.Müller, IKP-KFA Annual Report 1994, p.72 (1995).

[25] N.Amaglobeli et al., IKP-KFA Annual Report 1993, p.55 (1994).

[26] M.Büscher et al., IKP-KFA Annual Report 1994, p.63 (1995).

[27] V.I.Komarov et al., IKP-KFA Annual Report 1993, p.57 (1994).

[28] A.Sibirtsev et al., Preprint of Giessen University, December 16, 1996

[29] W.Oelert, *private communication.*

[30] A.K.Kacharava et al., NIM **A 376** p.356 (1996)